J. Membrane Biol. 54, 203–212 (1980)

The Journal of
Membrane Biology

Distribution and Diffusion of Alamethicin in a Lecithin/Water Model Membrane System

Urs Peter Fringeli

Laboratory for Physical Chemistry, Swiss Federal Institute of Technology, CH-8092 Zurich, Switzerland

Summary. Attenuated total reflection infrared spectroscopy has been used to determine the equilibrium distribution of the peptide antibiotic alamethicin R_F30 between dipalmitoyl phosphatidylcholine bilayers and the aqueous environment. The distribution coefficient $K = c_{eq}^W/c_{eq}^M$ turned out to be concentration dependent, pointing to alamethicin association in the membrane with increasing concentration in the aqueous phase (c_{eq}^W). This concentration was varied within 28 and 310 nM, i.e., in a range typical for black film experiments. Furthermore, diffusion coefficients of alamethicin in the hydrophobic phase of the membrane (D_M) and across the membrane/water interface (D_I) have been estimated from the time course of the equilibration process. It was found that the diffusion rate of the uncharged analogue R_F50 is about 10 times higher than that of the R_F30 component, exhibiting one negative charge at the *C*-terminus. The time constants for transmembrane diffusion of alamethicin R_F30 varied between 2.2 hr at low concentration and 3.2 hr at higher concentration. The corresponding low concentration value of the R_F50 component was found to be 0.25 hr.

Alamethicin (ALA) is an antibiotic isolated from *Trichoderma viride*. When ALA is added to lipid bilayer membranes in nano- to micromolar concentrations, pore formation is observed under the influence of a properly applied electric potential across the membrane. The reader is referred to Boheim and Kolb (1978) for a review of electrical and kinetic phenomena. The peptide is linear and consists of 19 amino acids (Gisin, Kobayashi & Hall, 1977), whereas 16 of them are hydrophobic. Concerning the molecular mechanism of pore formation, most models presented so far are based on the assumption that ALA is adsorbed at the membrane/water interface. Insertion of ALA into the membrane is reported to occur under the influence of an electric field (Boheim & Kolb, 1978). This molecular mechanism was derived predominantly from kinetic data of membrane conductance measurements, i.e., from information on a macroscopic level. Alternatively, Fringeli and Fringeli (1979) have recently shown by means of attenuated total reflection (ATR) infrared (IR) spectroscopy that in the absence of an electric field ALA is already located predominantly in the hydrophobic phase of the bilayer membrane and not adsorbed at its interface. Therefore, in equilibrated membranes field-induced pore formation cannot be initiated by insertion of peptide molecules from the hydrophilic surface into the interior of the membrane, as commonly was assumed. This paper investigates the similarities between the experimental conditions used in ATR-IR studies of ALA interaction with dipalmitoyl phosphatidylcholine (DPPC) bilayers and those commonly used with black lipid membranes. For that purpose the equilibrium distribution of ALA between the bilayer membrane and the surrounding aqueous phase as well as the diffusion coefficients of ALA in DPPC double layers and across the DPPC/water interface were determined. The former results in typical ALA equilibrium concentrations in the aqueous phase and in the membrane. From the latter it can be estimated whether the black lipid membrane has already reached ALA equilibrium concentration during the performance of conductance experiments. Concerning membrane fluidity, it should be noted that black film experiments are generally performed with lipids, whose gel-to-liquid crystalline phase transition is below 25 °C. This is not the case for DPPC, whose transition temperature is at ~41 °C. However, incorporation of ALA into DPPC bilayers leads to a significant reduction of hydrocarbon chain ordering in aqueous environment, i.e., enhancement of membrane fluidity with respect to pure DPPC (Fringeli &

0022-2631/80/0054-0203 $02.00

Fringeli, 1979). There is good evidence that the data reported in this paper may approximately be applied to black lipid membranes, too (*cf. Conclusions*).

Materials and Methods

L-α-dipalmitoyl phosphatidylcholine (DPPC) was obtained from R. Berchtold, Biochemical Laboratory, Mattenhofstrasse 34, CH-3007 Bern. Alamethicin $R_F 30$ (ALA $F30$) and alamethicin $R_F 50$ (ALA $F50$) were kindly provided by Dr. G.B. Whitfield, Upjohn Co., Kalamazoo, Mich., and Prof. G. Jung, University of Tübingen, D-7400 Tübingen, respectively. The internal reflection plates were obtained from Harrick Scientific Corp., Croton Dam Road, Ossining, N.Y. 10562. Concerning attenuated total reflection infrared (ATR-IR) spectroscopy, the reader is referred to Harrick (1967) and to Fringeli (1977).

For membrane formation, some drops of the stock solution in chloroform (DPPC: $10^{-2}-10^{-3}$ M; molar ratio $n_{DPPC}/n_{ALA}=50$) were homogeneously spread by means of a glass bar on one or on both sides of a zinc selenide ATR plate ($50\times10\times1$ mm, trapezoid, $\theta_0=45°$). Multibilayers were formed by evaporation of the solvent while the bar was slowly moved along the surface of the plate. This technique resulted in oriented layers with domains of uniform interference colors, i.e., uniform thickness, of about 1 cm^2, depending on the amount of substance used for membrane formation. The actual area of the membrane was 2.8 or 5.6 cm^2, depending on whether it was attached to one or both sides of the ATR plate. DPPC and DPPC/ALA model membranes have turned out to be stable over periods of observation much longer than those typical for this work, i.e., there occurred no structural rearrangements as observed, e.g., with oriented layers of tripalmitin (Kopp et al., 1975, 1976) and some phospholipid analogues (Fringeli, 1977). However, it should be noted that both evaporation of solvent without spreading by a glass bar and fast evaporation of the solvent lead to layers with inhomogeneous thickness and crystallization, respectively. Such layers are opaque and therefore have not been used as model membranes.

A prerequisite for the incorporation of ALA into the lipid membrane is its exposure to liquid water (Fringeli & Fringeli, 1979). Incorporation can be achieved to a considerable extent by overlaying the membrane with a thin film of water (~20 µl/cm^2) for about 1 hr followed by drying with a clean air stream (~70% rel. humidity at 25 °C). After this treatment the ATR plate was mounted in the cell holder. The amounts of ALA and DPPC were determined by means of the integrated intensity ($-\int \ln T(\tilde{\nu})\,d\tilde{\nu}$: interval of integration 1600–1700 cm^{-1}) of the amide I band, and by the peak intensity ($\alpha_{max}=-\ln T_{min}$) of the α-$CH_2$-bending vibration ($\delta(\alpha\text{-}CH_2)$) of DPPC hydrocarbon chains at 1420 cm^{-1}, respectively. The latter band was selected because its intensity remains practically unaffected by conformational changes of the hydrocarbon chains. Concerning the amide I band, the use of integrated intensities turned out to be more adequate because shape and position of the band critically depend on the degree of ALA incorporation into the DPPC bilayers (Fringeli & Fringeli, 1979). The transition dipole moment of amide I, however, was found to remain unaltered within the experimental error. The sample was heated up to 50 °C for intensity measurements in order to avoid disturbance of the amide I band intensity by the OH-bending vibrations of water. Furthermore, the base line of amide I was determined by comparison with ATR-IR spectra of pure DPPC measured under the same conditions (50 °C, dry N_2). The determination of the surface concentrations of ALA and DPPC was performed by means of Eqs. (1) and (2). Afterwards the temperature was decreased to 25 °C and a given volume (2–10 ml) of pure water was pumped in a close cycle through the ATR-cell by means of a peristaltic pump (1 ml/min; flow rate in the cell: 0.7 cm/sec) for a given period. Then the cell was poured out completely. A wet nitrogen flow (~90% rel. humidity at 25 °C) was fed to the ATR cell while it was heated up again to 50 °C. The sample was kept at 50 °C for another 30 min in the wet atmosphere before complete drying was performed in a dry nitrogen flow. This procedure enabled reformation of the ALA helix typical for dry membranes from the extended, membrane spanning conformation, typical in aqueous environment (Fringeli & Fringeli, 1979). After scanning the polarized ATR-IR spectra, the same volume of water (now already containing ALA dissolved from the membrane) was reused for circulation. The whole procedure was continued until the equilibrium distribution was reached. Typical examples are shown in Figs. 1 and 2.

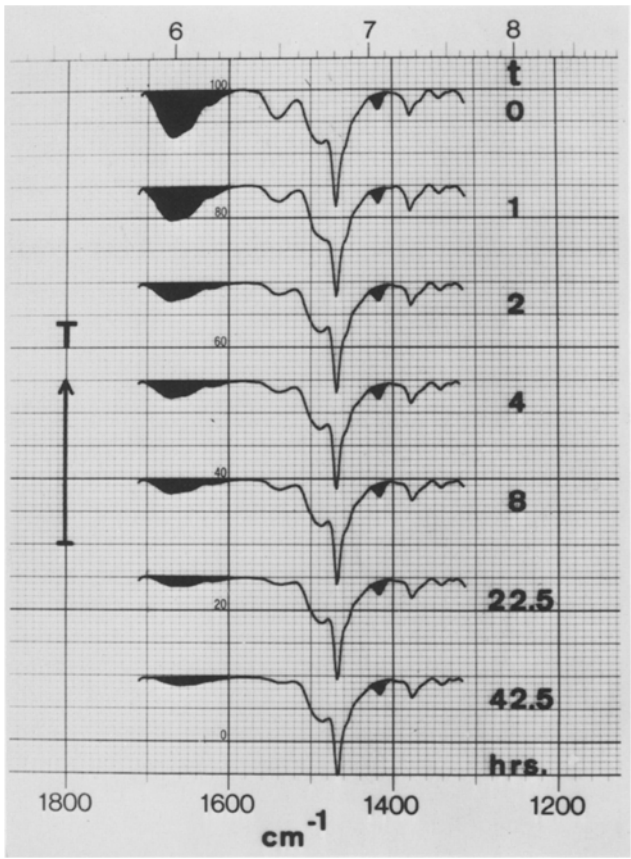

Fig. 1. Typical series of ATR-IR spectra scanned during the equilibration process. The amounts of ALA and DPPC have been determined by means of the amide I band (1660 cm^{-1}) and the α-methylene bending vibration of hydrocarbon chains (1418 cm^{-1}), respectively. The membrane has been dried after each period of liquid water exposure at 25 °C and heated up to 50 °C for the measurement (dry N_2 stream, parallel polarized incident light). Data evaluated from this series are presented in Fig. 2

Finally it should be noted that 2.8×10^{-10} or 4.7×10^{-10} moles of ALA were found to adsorb to the walls of the ATR cell (Teflon and glass) and/or to the walls of the tubes (silicon and Teflon), depending on the set-up used. This effect could be avoided when wall adsorption was saturated by a short circulation of about 50 nM ALA before starting the experiment. Cleaning of the set-up with alcohol reactivated the walls for ALA adsorption.

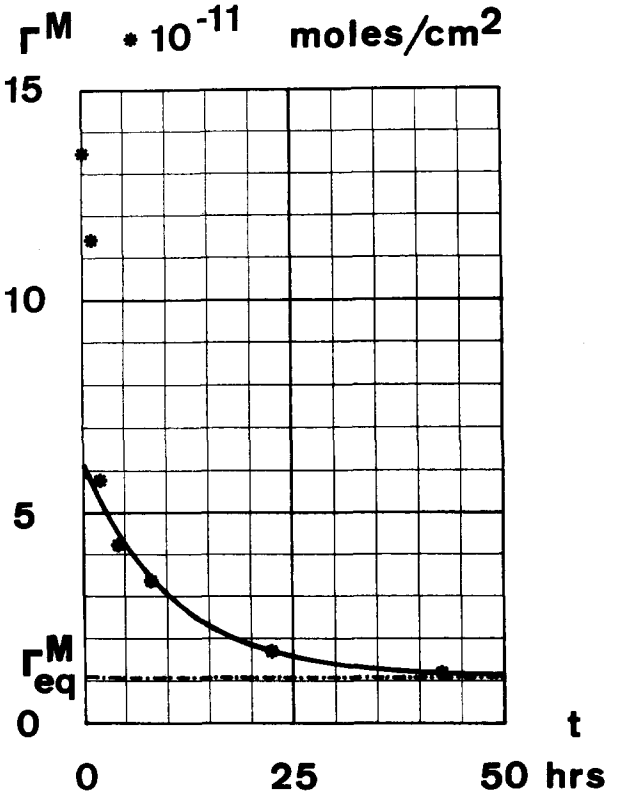

Fig. 2. Typical plot of ALA surface concentration Γ^M as determined by Eqs. (1) and (2) against the time of liquid water exposure at 25 °C. The fast decrease during the first two hours results from ALA F50 exhibiting a diffusion rate about 10 times higher than that of ALA F30. The solid line is obtained by a least squares fit according to Eq. (13). It levels off at the equilibrium surface concentration Γ^M_{eq}. Mean thickness of the membrane: 5.8 bilayers

The ATR-IR spectra were digitized by means of a Summagraphics Mod. ID-2-CTR-17 digitizer interfaced to a WANG 2200 MVP computer.

Theory

Determination of Surface Concentrations

Because the IR field strength in the rarer medium is anisotropic, i.e., $E_x \neq E_y \neq E_z$ and decreases exponentially with the distance from the surface of the ATR plate (Harrick, 1967; Fringeli, 1977), the determination of concentrations becomes somewhat more complicated than in conventional transmission technique. Equations (1) and (2) have been derived under the following conditions:

i) Weak absorption per internal reflection
ii) Microcrystalline ultrastructure
iii) Homogeneous layer thickness ℓ and homogeneous concentration distribution within the layer
iv) Layer thickness ℓ small compared with the penetration depth d_p. The exponential decay of the field strength $E(z) = E_o \cdot \exp(-z/d_p)$ may be approximated by $E(z) = E_o \cdot (1 - z/d_p)$.

Conditions i–iv are adequately fulfilled by the model membranes used in this work. More details concerning the derivation of Eqs. (1) and (2) as well as of corresponding expressions applicable to layers with liquid crystalline ultrastructures will be published elsewhere.

For parallel (∥) polarized incident light one obtains

$$\Gamma^M = \frac{2\alpha_{\parallel} \cdot [2d_p/(2d_p - \ell)]^2}{\mu_o^2 \cdot N_A \cdot v \cdot R \cdot \{E_{ox}^2 [ST(1 - \frac{3}{2}SG) + SG] + 2E_{oz}^2 [CT(1 - \frac{3}{2}SG) + \frac{1}{2}SG]\}} \quad (1)$$

and for perpendicular (⊥) polarized incident light

$$\Gamma^M = \frac{2\alpha_{\perp} [2d_p/(2d_p - \ell)]^2}{\mu_0^2 \cdot N_A \cdot v \cdot R \cdot E_{oy}^2 [ST(1 - \frac{3}{2}SG) + SG]} \quad (2)$$

where

Γ^M = Surface concentration (moles/cm^2).
$\alpha_{\parallel,\perp}$ = Absorption of ∥- and ⊥-polarized light, respectively. ($\alpha = -\ln T_{min}$ or $\alpha = -\int \ln T(\tilde{\nu})\, d\tilde{\nu}$, when peak absorptions (α_{max}) or integrated absorptions are used for concentration determination, respectively.)
μ_o^2 = Normalized absorption coefficient per reflection, per functional group and per area (refl.$^{-1}$ · funct. group^{-1} · cm^{-2}).
N_A = Avogadro's number = 6.02×10^{23} molecules/mole.
v = Number of equivalent functional groups per molecule.
R = Number of internal reflections in the ATR plate.
ℓ = Mean thickness of the total membrane layer.
d_p = Penetration depth of the electric field with wavelength λ into the rarer medium:
$d_p = (\lambda/n_1)/[2\pi(ST - (n_3/n_1)^2)^{1/2}]$
$n_{1,3}$ = Refractive indices of the reflection plate (1) and the bulk rarer medium (3), respectively.
$ST = \sin^2\theta$; θ = angle of incidence of the IR beam with respect to the ATR plate.
$CT = \cos^2\theta$; *cf.* ST.
$SG = \sin^2\gamma_o$; γ_o = angle between transition dipole moment and the normal (z-axis) of the ATR plate.
E_{ox}, E_{oy}, E_{oz} = x-, y- and z-components of the electric field strength at the surface of the ATR plate (rarer medium, weak absorption, *cf.* Harrick, 1967; Fringeli, 1977).

Determination of Diffusion Coefficients

(i) Ultrastructural Model. First, multibilayers attached to the ATR plate are assumed to have homo-

geneous thickness. This assumption is fulfilled for domains with an area up to 1 cm^2 (*see* above), whereas in our experiments the total surface was 2.8 or 5.6 cm^2. The variance of the mean thickness of the multilayer membrane is estimated to be in the order of 10% as concluded from the reproducibility of the kinetics of ALA dissolution from the initial DPPC/ALA membrane during the equilibration procedure (Fig. 2).

Second, the multibilayer membrane system used in this work may be described by a model of succesive parallel plates, $MWMW\ldots MWB$, where M, W and B denote lipid bilayer membrane, aqueous layer between successive lipid bilayers, and bulk aqueous phase, respectively. Diffusion of substance A across these parallel plates may be described by 3 diffusion coefficients D_M, D_I and D_W, denoting diffusion in the interior of the bilayer membrane (hydrophobic region), diffusion across the membrane/water interface, and diffusion in the aqueous phase, respectively.

(ii) Simplified Model for Solution of Diffusion Problem. The ultrastructural model $MWMW\ldots MWMB$ described in section (*i*) above consisting of n lipid bilayers (M) and $n-1$ water layer (W) may be simplified to a two-plate model $M'B$, where M' denotes a plate with n times the thickness of M, and B denotes the bulk aqueous phase. This approximation is adequate under the assumption of a local equilibrium between ALA in the water layer i and ALA incorporated from this layer into the lipid bilayers i and $i+1$. The amount of ALA required to reach equilibrium concentration in the aqueous layer i is easily supplied by the lipid bilayer i and $i+1$ because, on the one hand, the volume of a water layer W is small, i.e., comparable to that of a lipid bilayer M, and, on the other hand, the distribution coefficient $K = c_{eq}^W / c_{eq}^M \cong 10^{-5}$ (for $c_{eq}^W \cong 30$ nM). No ALA transfer across the bilayers is required to establish this equilibrium. Consequently, one may assume that the ALA concentrations in the facing membrane surfaces i and $i+1$ (i.e., the number of ALA molecules per area, incorporated from aqueous phase i) are approximately the same. In this case, however, the water layer W in the ultrastructural model $MWMW\ldots MWMB$ may be neglected, resulting in a simplified model $M'B$. It should be noted that there is some experimental evidence for approximate local equilibrium between membranes $i/i+1$ and the water layer i, at least during an initial period of the experiment. Equilibration experiments described below show that the ALA flux into the bulk water phase (B) decreases exponentially with time (Fig. 2). The time constant τ of this process is directly proportional to the mean number $\bar{n}$ of lipid double layers, i.e., $\tau = \bar{n} \cdot \tau_o$, where τ_o denotes the time constant for ALA transfer across a single bilayer membrane (*cf.* Table 1). Now, if water is added to a dry, equilibrated membrane (ALA only dissolved in M, *cf.* Fringeli & Fringeli, 1979) two ALA fluxes must be considered, first the flux across the surface of the n-th membrane into the bulk water phase (B), given by

$$J^B(\ell - o, t) = \frac{\ell}{\tau}(c_o^M - c_{eq}^M)\, e^{-\frac{t}{\tau}} = \frac{\ell_o}{\tau_o}(c_o^M - c_{eq}^M)\, e^{-\frac{t}{\bar{n}\tau_o}} \quad (3)$$

Table 1. ALA distribution and diffusion in DPPC bilayers: Aqueous environment at 25 °C[a]

Substance	Γ_{eq}^{ob} (moles/cm^2)	K^c	τ^d (hr)	$\bar{n}^e$ (bilayers)	$\tau_o = \tau/\bar{n}^f$ (hr)	$D_M/D_I{}^g$ (cm)	$D_M{}^h$ (cm^2/sec)	$D_I{}^i$ (cm/sec)	$\tau_M{}^j$ (hr)
ALA F30	8.4×10^{-12}	4.17×10^{-6}	48.8	15.65	3.12	$\geqq 2.09\times10^{-12}$	$\geqq 3.0\times10^{-17}$	$\leqq 1.4\times10^{-5}$	$\leqq 1.2$
ALA F30	7.7×10^{-12}	3.95×10^{-6}	90.9	28.63	3.18	$\geqq 1.98\times10^{-12}$	$\geqq 3.0\times10^{-17}$	$\leqq 1.5\times10^{-5}$	$\leqq 1.2$
ALA F30	1.1×10^{-12}	9.76×10^{-6}	8.8	3.38	2.60	$\geqq 4.88\times10^{-12}$	$\geqq 3.6\times10^{-17}$	$\leqq 7.4\times10^{-6}$	$\leqq 0.95$
ALA F30	7.6×10^{-13}	1.03×10^{-5}	12.9	5.76	2.24	$\geqq 5.15\times10^{-12}$	$\geqq 4.2\times10^{-17}$	$\leqq 8.2\times10^{-6}$	$\leqq 0.83$
ALA F50	1.7×10^{-12}	$\sim10^{-5}$	1.67	6.83	0.245	$\geqq 5\times10^{-12}$	$\geqq 3.8\times10^{-16}$	$\leqq 7.6\times10^{-5}$	$\leqq 0.091$ (5.5 min)

[a] The statistical error of all data is $<10\%$. However, there could be a shift up to 20% resulting from systematic errors of μ_o^2 and of E_{ox}^2, E_{oy}^2, E_{oz}^2, respectively (*cf.* Eqs. (1) and (2))

[b] ALA surface concentration per monolayer (*cf.* Fig. 3).

[c] Distribution coefficient (*cf.* Eq. (17)).

[d] Time constant for ALA diffusion across $\bar{n}$ DPPC bilayers (*cf.* Eq. (13)).

[e] Mean number of DPPC bilayers determined by means of $\delta(\alpha\text{-}CH_2)$ and Eqs. (1), (2), and (14)–(16) (weighted mean, taking DPPC loss during the experiment into account).

[f] Time constant for ALA diffusion across one bilayer. ALA diffusion along the water layer between successive DPPC bilayers can be neglected, i.e., $\tau_o = \tau/\bar{n}$

[g] $D_M/D_I \geqq K \cdot \ell_o$ (*cf.* Eq. (10)).

[h] Diffusion coefficient of ALA across the hydrophobic region of the bilayer (*cf.* Eqs. (9) and (11)).

[i] Film diffusion coefficient of ALA at the membrane water interface (ALA incorporation) related to D_M^{min}.

[j] Mean transfer time for ALA diffusion across the hydrocarbon chain region of the bilayer membrane (*cf.* Eq. (12)).

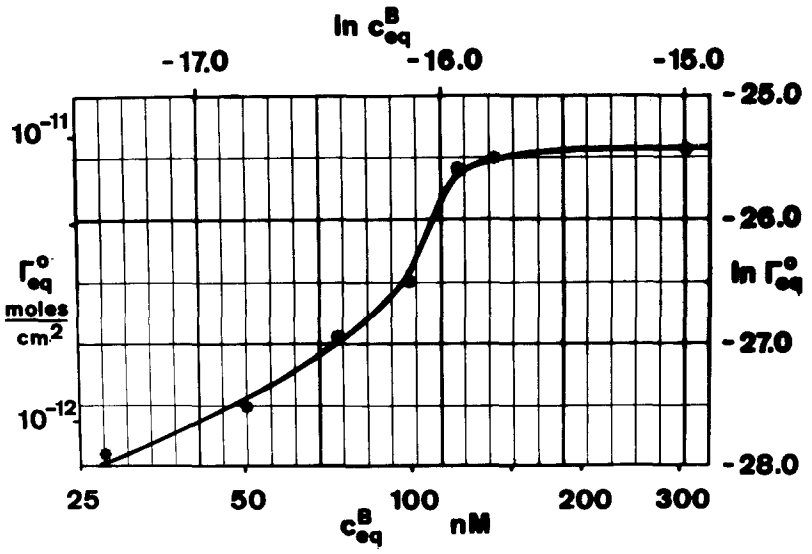

Fig. 3. Double logarithmic plot of ALA F30 surface concentration per DPPC monolayer against the ALA F30 concentration in the aqueous phase. The equilibration process has been performed at 25 °C. The statistical error of Γ^o_{eq} and c^B_{eq} is $<10\%$. However, values could be shifted up to 20% due to systematic errors of μ_0^2, E^2_{ox}, E^2_{oy} and E^2_{oz}, respectively. (*cf.* Eqs. (1) and (2))

and second, the flux of ALA from the i-th and $(i+1)$-th bilayer into the water layer i (W) between them, approximated by

$$J^W(i\cdot\ell_o, t)\cong\frac{\ell_o}{\tau_o}(c^M(i\cdot\ell_o, t)-c^M_{eq}(i\cdot\ell_o, t))\cdot e^{-\frac{2t}{\tau_o}} \qquad (4)$$

where ℓ and ℓ_o denote the total thickness of the multilayer membrane, and the thickness of one bilayer, respectively, c^M_o and c^M_{eq} are the initial and equilibrium concentrations of ALA in the multilayer membrane. Concerning Eq. (4), $c^M(i\cdot\ell_o, t)$ and $c^M_{eq}(i\cdot\ell_o, t)$ denote the mean ALA concentration in the i-th bilayer and the corresponding equilibrium concentration with respect to ALA dissolution into water layers i and $i-1$. On the other hand, Eq. (4) is also an approximate description of the ALA flux from membranes i and $i+1$ into the water layer i. Because $c^M(i\cdot\ell_o, t)$ decreases with time constant $n\cdot\tau_o$(Eq. (3)), one should assume that an approximate local equilibrium between membranes $i/i+1$ and the water layer i is adequate. This process has a time constant of $\sim\tau_o/2$, at least during the initial period of the experiment (Eq. (4)). However, one may assume that local equilibrium is approximately maintained for the whole period of observation; i.e., the simplified diffusion model $M'B$ consisting of a hydrophobic plate M', exhibiting a hydrophilic surface in contact with an aqueous plate B, may be used tentatively. The more adequate model *MWMW... MWMB*, taking the multilayered membrane ultrastructure into account, will be discussed elsewhere. Finally, it should be mentioned that lateral diffusion of ALA in the water layer can be neglected in these experiments, because of the experimental finding $\tau=\bar{n}\cdot\tau_o$ (*cf.* Eq. (3) and Table 1).

(iii) Boundary Conditions and Solution of Diffusion Problem. Diffusion of ALA is considered to be perpendicular to the membrane surface (z-axis of coordinate system). The membrane M' has a thickness $\ell=\bar{n}\cdot\ell_o$(ℓ_o=thickness of one bilayer, $\bar{n}$=mean number of bilayers). The inner surface of M' attached to the ATR plate is impermeable. The bulk water phase B is well stirred in order to obtain homogeneous distribution of ALA concentration. Denoting $c^M(z, t)$ and $c^B(t)$ as the ALA concentrations in the membrane M' and the aqueous phase, respectively, the following boundary conditions may be stated:

$$\begin{aligned}
c^M(z, 0) &= c^M_o, & 0<z<\ell\\
c^B(z, 0) &= c^B(t=0)=0, & z>\ell\\
c^M(z, \infty) &= c^M_{eq}, & 0<z<\ell\\
c^B(z, \infty) &= c^B(\infty)=c^B_{eq}, & z>\ell.
\end{aligned}$$

The Nernst distribution coefficient is given by

$$K=c^B_{eq}/c^M_{eq}.$$

The ALA flux through the membrane/water interface is then given by

$$\begin{aligned}
J^B(\ell-o, t) &= -D_M\left(\frac{\partial c^M(z, t)}{\partial z}\right)_{\ell-o}\\
&= -D_I(c^B(t)-K\cdot c^M(\ell-o, t)). \qquad (5)
\end{aligned}$$

A considerable number of solutions of differential equations dealing with heat conduction problems is reported by Carslaw and Jaeger (1959). The mathematical solutions for slabs with a radiation boundary condition can easily be transformed to the corresponding problems of mass diffusion with Nernst distribution. Concerning Eq. (5), the solution of the

special case $c^B(t)=0$, i.e., the ATR cell is rinsed out with water saturated by DPPC, is found to be

$$\frac{c^M(z,t)}{c_o^M}=\sum_{k=1}^{\infty}\frac{2\ell\cdot\frac{D_I\cdot K}{D_M}\cdot\cos\left(\alpha_k\cdot\frac{z}{\ell}\right)\cdot\sec\alpha_k}{\ell\frac{D_I\cdot K}{D_M}\left(\ell\frac{D_I\cdot K}{D_M}+1\right)+\alpha_k^2}\cdot e^{-\frac{\alpha_k^2\cdot D_M}{\ell^2}\cdot t} \quad (6)$$

where α_k denotes the k-th positive root of the transcendental equation

$$\alpha\cdot tg\,\alpha=\ell\cdot\frac{D_I\cdot K}{D_M}. \quad (7)$$

Because on the one hand $\ell\ll\lambda_{IR}$ (λ_{IR} = infrared wavelength), and on the other hand $c^B(t)$ is too small for IR spectroscopic detection ($0\leqq c^B\leqq 300$ nM), ATR-IR experiments reveal direct information on the average ALA concentration in the membrane. Averaging Eq. (6) results in

$$\frac{c_{av}^M(t)}{c_0^M}=\sum_{k=1}^{\infty}\frac{2\left(\ell\frac{D_I\cdot K}{D_M}\right)^2}{\alpha_k^2\left[\ell\cdot\frac{D_I\cdot K}{D_M}\left(\ell\frac{D_I\cdot K}{D_M}+1\right)+\alpha_k^2\right]}\cdot e^{-\frac{\alpha_k^2\cdot D_M}{\ell^2}\cdot t}. \quad (8)$$

Experimental results (Fig. 4) show that $c_{av}^M(t)$ may be fitted by a single exponential decay within the experimental error, i.e., the eigenvalue α_1 is dominant, and one obtains from Eq. (8)

$$\frac{c_{av}^M(t)}{c_0^M}=\frac{2\left(\ell\frac{D_I\cdot K}{D_M}\right)^2}{\alpha_1^2\left[\ell\cdot\frac{D_I\cdot K}{D_M}\left(\ell\frac{D_I\cdot K}{D_M}+1\right)+\alpha_1^2\right]}\cdot e^{-\frac{\alpha_1^2\cdot D_M}{\ell^2}\cdot t}. \quad (9)$$

Furthermore, the dominance of α_1 leads to the inequalities (Carslaw & Jaeger, 1959)

$$\ell\cdot\frac{D_I\cdot K}{D_M}\leqq 1 \quad (10)$$

and

$$\alpha_1\leqq 0.86. \quad (11)$$

Equations (9)–(11) may now be used to estimate D_M and D_I, i.e., the ALA diffusion coefficient across the hydrophobic part of the membrane, and the film diffusion coefficient, respectively. Finally, if D_M is known, the mean time τ_M required for ALA transfer across the hydrophobic region of a bilayer membrane with thickness ℓ_0 can be calculated by means of the Einstein-Smoluchowsky relation $D=z^2/2t$. Thus

$$\tau_M=\ell_o^2/2D_M. \quad (12)$$

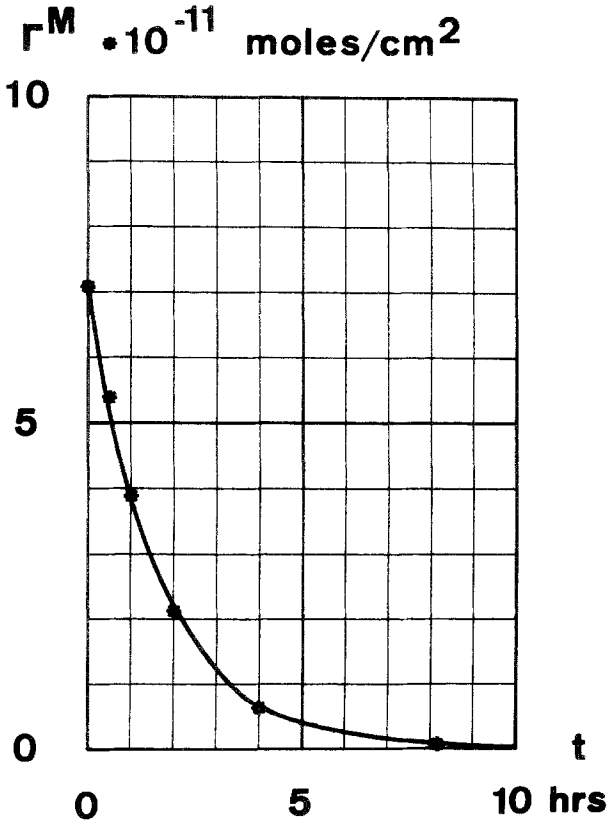

Fig. 4. Time course of ALA F50 dissolution from a DPPC/ALA F50 model membrane by pure, DPPC saturated water. 25 °C, mean thickness of the membrane: 6.8 bilayers

Results and Discussion

(i) Equilibrium Distribution and Equilibration Kinetics

Figure 1 shows parallel polarized ATR-IR spectra scanned during the equilibration process described in a previous section. The spectra are normalized with a base line determined from a corresponding spectrum of pure DPPC in order to obtain amide I bands ($\sim 1660\,cm^{-1}$, free of overlapping by the intense carbonyl stretching mode ($\nu(C=0)$) of DPPC near $1740\,cm^{-1}$. The surface concentrations of ALA and DPPC have been determined by means of Eqs. (1) and (2). Integrated normalized absorption coefficients have been used with the amide I band (μ_0^2(amide I, 1600–$1700\,cm^{-1}$, 50 °C) $=(1.0\pm 0.1)\times 10^{-16}\cdot$ functional group$^{-1}\cdot$ reflection$^{-1}\cdot cm^{-2}$), and normalized peak absorption coefficients have been used with the

α-methylene bending mode of the fatty acid chains of DPPC ($\mu_0^2(\delta(\alpha\text{-}CH_2), 50\,°C) = (2.75 \pm 0.10) \times 10^{-19}$ · functional group^{-1} · reflection^{-1} · cm^{-2}), respectively (*cf. Materials and Methods*). Figure 1 demonstrates also that the mass loss of DPPC due to membrane detachment during water circulation is small (generally $< 10\%$ over a period of 50–100 hr). Nevertheless, the surface concentrations of ALA plotted against the time of water exposure (Fig. 2) have been corrected with respect to DPPC mass loss.

The results presented in Figs. 1 and 2 were obtained from a DPPC/ALA F30 membrane with an initial molar ratio of 47.8:1 and a mean thickness of 5.8 bilayers. Figure 2 can be used to determine the equilibrium surface concentration (Γ_{eq}^M) of ALA, and the corresponding ALA concentration in the aqueous phase, provided that the membrane surface and the volume of the bulk water phase are known. Figure 2 can furthermore be used to estimate the bulk membrane diffusion coefficient, D_M, and the film diffusion coefficient, D_I (*see* above). However, if Eqs. (6), (8) or (9) should be applied, Fig. 2 has to be adapted to the case, where the ALA concentration in the bulk water phase B is zero ($c^B(t) = 0$). Alternatively, Eqs. (6), (8) and (9) can directly be applied to experimental data as presented in Fig. 4. In this case, $c^B(t)$ was set at zero by rinsing out the ATR cell with a continuous, DPPC-saturated flow of water (*see* below).

The solid curve in Fig. 2 is obtained by a least squares analysis of experimental data with

$$\Gamma^M(t) = \Gamma_{eq}^M + (\Gamma^M(0) - \Gamma_{eq}^M) e^{-t/\tau}. \quad (13)$$

Evidently, the calculated curve fits well for $t > 2$ hr. There are two possible explanations for the fast decay observed for $t < 2$ hr. Firstly, in the mathematical solution of the diffusion problem, Eqs. (6) and (8), one has also to consider higher-order terms, e.g., the 2nd positive root α_2 of Eq. (7) (α_2 is always $> \alpha_1$). Secondly, the ALA F30 sample was not pure, but contained about 50% wt. of a second peptide. If the latter interpretation is true, it should easily be possible to separate the two peptides because their diffusion coefficients differ by a factor of about 10. Separation of the components was indeed possible, if the ATR cell, containing a freshly prepared ALA F30/DPPC membrane, was rinsed out for an adequate time (at least 2 hr for a sample corresponding to Fig. 2). After this procedure a single exponential decrease of ALA concentration in the membrane is found during the equilibration process (*cf.* Fig. 4). This experiment proves that only the first positive root of Eq. (7) is dominant. Exchange of Glu^{18} in ALA F30 by Gln^{18} results in the analogue ALA F50.

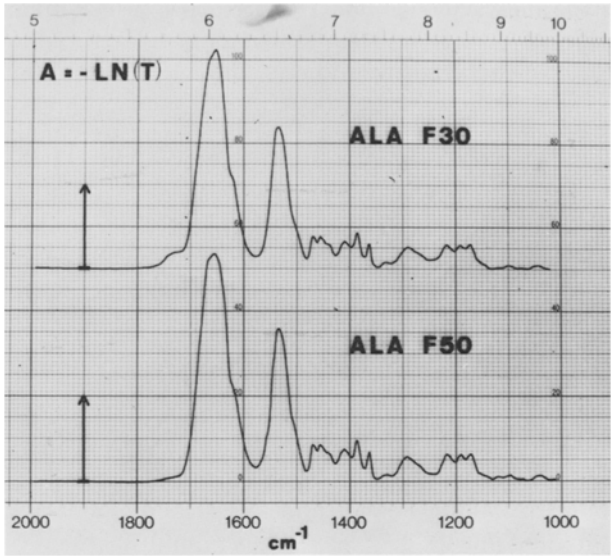

Fig. 5. Comparison of the ATR-IR spectra of ALA F30 and ALA F50 in the $2000 - 1000\,cm^{-1}$ region. The exchange of Glu^{18} by Gln^{18} leads to a disappearance of the carbonyl stretching absorption band at $1730\,cm^{-1}$, and to a weak broadening of the amide I band due to $-CONH_2$ absorption (ALA F50)

This peptide antibiotic is also produced by *Trichoderma viride* (Irmscher & Jung, 1977). ALA F50 also shows a single exponential decay curve in the diffusion experiment, however, with a striking decrease of the time constant τ (*cf.* Eqs. (3), (4), (13) and Fig. 4). τ was found to be about 10 times smaller than for ALA F30. On the other hand, if the ATR-IR spectra of ALA F30 and ALA F50 are compared (Fig. 5 *a, b*), there are only weak differences in the $1700\,cm^{-1}$ region (ν(COOH)) and in the shape of the amide I band ($1650\,cm^{-1}$). Both effects result from the exchange of Glu^{18} by Gln^{18} mentioned above. Therefore one has to conclude, that ~ 50 wt.% impurity detected in ALA F30 used in this work must result from its analogue ALA F50. Otherwise the close similarity of the IR spectra presented in Fig. 5 could not be explained. Fig. 3 shows a plot of the logarithm of ALA equilibrium surface concentration calculated per DPPC monolayer ($\ln \Gamma_{eq}^o$) against the logarithm of the corresponding ALA concentration in the aqueous phase ($\ln c_{eq}^B$). It should be noted that c_{eq}^B determined from $\Gamma^M(0)$, Γ_{eq}^M, the membrane surface and the volume of the aqueous phase has to be corrected for ALA adsorption in the ATR-cell and in the tubes, unless these walls have been saturated before starting the experiment (*cf. Materials and Methods*). In the case of Fig. 2, wall adsorption had to be taken into account with 4.7×10^{-10} moles.

The initial slope of the $\ln \Gamma_{eq}^o$ *vs.* $\ln c_{eq}^B$ curve (Fig. 3) is 1. It increases with increasing ALA concentration

in the bulk aqueous phase and reaches a maximum value of 3–6 at 110 nM. Above this concentration there is sudden saturation of the membrane. The increase of the slope at low ALA concentrations may be explained by the formation of dimers and multimers in the membrane, a process that is favored by increasing surface concentration of ALA. In a variety of earlier work, it has been reported that membrane conductivity increases with a higher power (up to 14.4) of ALA concentration in the aqueous phase. This effect was also explained with the formation of multimers (for a review *cf.* Boheim & Kolb (1978) and Boheim, Irmscher & Jung (1978)). However, when the latter results are compared with those reported in this paper, one should be aware that here the surface concentration has been considered instead of the membrane conductance. Furthermore, black film experiments generally require lipid membranes consisting of a considerable amount of unsaturated hydrocarbon chains and an aqueous environment with electrolyte concentrations between 0.1 and 1.0 M. However, the experiments reported here have been performed with saturated hydrocarbon chains (DPPC) and without any salt in the aqueous phase.

Finally, it should be noted that the molar ratio DPPC/ALA at equilibrium varied from 555:1 at $c^B_{eq} = 28$ nM to 52:1 at 310 nM.

(ii) Estimation of Diffusion Coefficients

Kinetic data obtained from different model membranes resulted in time constants τ of the equilibration process (*cf.* Eq. (13)). Division of τ by the corresponding weighted mean number of bilayers $\bar{n}$ resulted in the time constant $\tau_0 = \tau/\bar{n}$, typical for ALA diffusion across one bilayer (*cf. Determination of Diffusion Coefficients*, Section (*ii*)). $\bar{n}$ is given by Eq. (14)

$$\bar{n} = \frac{\bar{\Gamma}_{DPPC}}{2\bar{\Gamma}^o_{DPPC}}. \tag{14}$$

$\bar{\Gamma}_{DPPC}$ denotes the mean DPPC surface concentration with respect to the experimental period and $\bar{\Gamma}^o_{DPPC}$ is the corresponding surface concentration per membrane monolayer. Taking the mean area requirements of ALA into account, one obtains

$$\bar{\Gamma}^o_{DPPC} = \frac{\bar{\Gamma}_{DPPC}}{N_A(\bar{\Gamma}_{DPPC} \cdot F_{DPPC} + \bar{\Gamma}_{ALA} \cdot F_{ALA})} \tag{15}$$

where N_A, F_{DPPC}, F_{ALA} and $\bar{\Gamma}_{ALA}$ denote the Avogadro's number, the area per DPPC and per ALA molecule, and the mean ALA surface concentration, respectively. Mean surface concentrations are calculated by means of Eq. (16)

$$\bar{\Gamma} = \frac{1}{2t_n} \cdot \sum_{i=2}^{n} (t_i - t_{i-1})(\Gamma_i + \Gamma_{i-1}). \tag{16}$$

n denotes the number of measurements performed during the equilibration process, and t_i is the time related to the surface concentration Γ_i.

If τ_o has been determined for a given membrane, the determination of the diffusion coefficients D_M and D_I, as well as of τ_M, the mean transfer time for ALA diffusing across the hydrophobic part of the bilayer membrane, is straightforward (*cf.* Eqs. (9)–(12)). The corresponding distribution coefficient K may be determined by means of Eq. (17) and Fig. 3.

$$K = c^B_{eq}/c^M_{eq} = c^B_{eq} \cdot \ell_o/2 \cdot \Gamma^o_{eq} \tag{17}$$

where c^B_{eq}, c^M_{eq}, ℓ_o and Γ^0_{eq} denote the ALA concentrations in the water phase (B) and the membrane (M), the thickness of a bilayer membrane, and the ALA surface concentration at equilibrium with respect to one monolayer, respectively. The results are presented in Table 1. They reveal three interesting facts. Firstly, the diffusion rate of ALA F50 across the membrane/water interface as well as across the hydrophobic phase of the membrane is about 10 times faster than that of its charged analogue ALA F30. Secondly, the comparison of τ_M and τ_o (Table 1) shows that the membrane/water interface must be considered as a significant barrier for ALA diffusion. One may tentatively relate the film diffusion coefficient D_I with the transport process of ALA from the aqueous phase into the membrane (or vice versa), whereas D_M could be related to the transport of ALA (including *C*-terminus) across the hydrophobic part of the membrane. Thirdly, there is a significant increase of τ_o with increasing ALA concentration paralleled by a corresponding decrease of the diffusion coefficient D_M and an increase of the film diffusion coefficient D_I. Equivalently, transmembrane diffusion is impeded on the one hand, and diffusion across the membrane/water interface is facilitated on the other hand. Both effects may be explained by the formation of dimers and multimers at elevated ALA concentrations. Finally, it should be mentioned that Jung et al. (1979) have reported data on erythrocyte hemolysis by a number of ALA analogues. They have found that ALA analogues without negative charge at the C-terminus (e.g., ALA F50, methylester of Trichotoxin A-40) result in hemolysis at a concentration about 10 times lower than their charged analogues. In the view of our results, one should assume that enhanced incorporation and/or transmembrane diffusion of uncharged ALA analogues are responsible for this effect.

Conclusions

Determination of the equilibrium distribution of ALA between membrane and aqueous phase has shown that the concentration range of ALA, typical for ATR-IR experiments, is between 25 and 300 nM in the aqueous phase.

This range is also typical for single-pore experiments with black lipid membranes (Boheim et al., 1978). Consequently, the ATR-IR finding that ALA is predominantly incorporated into the bilayer membrane (Fringeli & Fringeli, 1979) and not adsorbed at the membrane surface (Boheim & Kolb, 1978) can be transferred to equilibrated black lipid membranes. On the other hand, the measurement of the time course of the equilibration process of a DPPC/ALA model membrane enabled the determination of the transfer time constant τ_o for ALA diffusion across a bilayer membrane as well as estimations of the diffusion coefficients of ALA for transfer of the membrane/water interface (D_I) and transfer of the hydrocarbon chain region (D_M). It turned out that the film diffusion effect is significant, i.e., the time required for ALA incorporation from the aqueous phase into the membrane is expected to be of the same order of magnitude as the mean transfer time τ_M for ALA diffusion across the hydrocarbon chain region of the bilayer membrane. The time constant for ALA diffusion across one bilayer membrane (τ_o) depends significantly on the electric charge on the ALA molecule. Uncharged ALA F50 resulted in $\tau_o^{50} = 0.245$ hr, and ALA F30 with the negative charge at the C-terminus resulted in $\tau_o^{30} = 2.24$ hr (*cf.* Table 1). In the view of this finding, one should assume that in many conductance experiments nonequilibrated black films have been used, especially when ALA has been added only to one compartment of the set-up. Furthermore, Table 1 reveals a significant dependence of the diffusion flux on the ALA concentration in the membrane. Reduction of D_M and enhancement of D_I at elevated ALA concentration point to an interaction between the ALA transmembrane diffusion flux with the process of ALA multimer formation in the membrane.

Concerning the transfer of our data to black lipid membranes, one should discuss two further differences in experimental conditions. Firstly, the enhanced membrane fluidity of black lipid membranes resulting from lipids with unsaturated hydrocarbon chains, and secondly, the use of 0.1–1 M aqueous salt solutions instead of pure water. However, the following arguments should show that a significant influence on our principal conclusions is unlikely.

(i) Membrane fluidity: Saturated hydrocarbon chains of DPPC are significantly disordered upon incorporation of ALA in aqueous environment (Fringeli & Fringeli, 1979), i.e., the membrane fluidity is enhanced with respect to pure DPPC bilayers under the same conditions. This fact has also been recognized in earlier Raman studies by Knoll (1978) who has found that DPPC/ALA/H_2O dispersions do not exhibit the first-order phase transition at 41 °C, which is characteristic for DPPC/H_2O dispersions.

Instead of that, continuous melting of the hydrocarbon chains was observed with increasing temperature already below 41 °C. Thus, there is rather a gradual and not a discontinuous difference in membrane fluidity between the membranes used in this work and those commonly used for black lipid membrane experiments. Furthermore, membrane fluidity was found to have no significant influence on the structure of ALA, as revealed by recent infrared-ATR measurements of ALA incorporated into L-α-dipalmitoleoyl phosphatidylcholine (*to be published*).

Further evidence for the similarity of our membrane system with corresponding black lipid membranes is obtained via the observation of transmembrane diffusion. In a recent paper, Schindler (1979) has studied the autocatalytic transport of the peptide antibiotics suzukacillin A (an ALA analogue) and ALA R_F30 across black lipid membranes. The antibiotic was added to the compartment with the negative pole of the applied electric potential; i.e., the membrane was initially in the nonconductive state. Nevertheless, channel formation could be observed a certain period after addition of the antibiotic. This fact, however, involves peptide diffusion across the membrane, because channel opening occurs only by aggregates incorporated into the membrane from the positive side. The transmembrane diffusion time of suzukacillin was reported to be in the order of a few minutes, whereas the time for ALA R_F30 diffusion was several times longer. This finding is in agreement with our results presented in Table 1. Furthermore, there is some evidence that suzukacillin A is an uncharged ALA analogue because its diffusion behavior is similar to that of ALA R_F50. As mentioned above, there is also a qualitative agreement of our diffusion data with results of a study of the hemolytic properties of a number of charged and uncharged ALA analogues by Jung et al. (1979).

(ii) Influence of ionic strength: Gordon and Haydon (1975) have shown by film balance experiments that the surface concentration of ALA in a spread lipid monolayer depends on the ionic strength in the subphase. It was found to be enhanced by a factor $\leqq 2$ when the ionic strength was increased from 0.2 to 2.0 M. Since our data are obtained in the absence of electrolyte, the surface concentrations reported above

may be slightly influenced upon addition of 0.1–1.0 M KCl (typical condition for black lipid membrane experiments with ALA and ALA analogues (Boheim et al., 1978). On the other hand, recent infrared-ATR experiments reveal that the molecular structure of ALA is not affected upon addition of 1 M KCl (*to be published*).

Therefore, one should conclude from (*i*) and (*ii*) that the conclusions drawn from the experimental data presented in this paper also hold for black lipid membrane experiments. Concerning the experimental technique used in this paper, it was demonstrated that ATR-IR spectroscopy offers a new and direct approach to the determination of equilibrium distributions and transmembrane diffusion time constants in biomembranes. Corresponding diffusion constants can be derived in the framework of the model described above. Application of ATR-IR technique for the determination of diffusion coefficients of liquids penetrating into a polymer film has earlier been reported by Trifonov et al. (1975).

I thank Mrs. M. Fringeli for skilful performance of the exacting experimental part of this work, and Prof. Dr. Hs.H. Günthard for valuable discussions. Financial support by the Swiss Federal Foundation (Proj. No. 3.192.0.77) and by the Emil Barel Foundation (F. Hofmann-La Roche, Basel) is gratefully acknowledged.

References

Boheim, G., Irmscher, G., Jung, G. 1978. Trichotoxin A-40, a new membrane-exciting peptide. Part B: Voltage-dependent pore formation in bilayer lipid membranes and comparison with other alamethicin analogues. *Biochim. Biophys. Acta* **507**:485

Boheim, G., Kolb, H.-A. 1978. Analysis of the multi-pore system of alamethicin in a lipid membrane. *J. Membrane Biol.* **38**:99

Carslaw, H.S., Jaeger, J.C. 1959. Conduction of Heat in Solids. Oxford at the Clarendon Press, London

Fringeli, U.P. 1977. The structure of lipids and proteins studied by attenuated total reflection (ATR) infrared spectroscopy. II. Oriented layers of a homologous series: Phosphatidylethanolamine to phosphatidylcholine. *Z. Naturforsch.* **32c**:20

Fringeli, U.P., Fringeli, M. 1979. Pore formation in lipid membranes by alamethicin. *Proc. Nat. Acad. Sci. USA* **76**:3852

Gordon, L.G.M., Haydon, D.A. 1975. Potential-dependent conductances in lipid membranes containing alamethicin. *Phil. Trans. R. Soc. London B* **270**:433

Gisin, B.F., Kobayashi, S., Hall, J.E. 1977. Synthesis of a 19-residue peptide with alamethicin-like activity. *Proc. Nat. Acad. Sci. USA* **74**:115

Harrick, N.J. 1967. Internal reflection spectroscopy. John Wiley & Sons, New York

Irmscher, G., Jung, G. 1977. Die hämolytischen Eigenschaften der membranmodifizierenden Peptidantibiotika Alamethicin, Suzukazillin und Trichotoxin. *Eur. J. Biochem.* **80**:165

Jung, G., Brückner, H., Oekonomopulos, R., Boheim, G., Breitmaier, E., König, W.A. 1979. Structural requirements for pore formation in alamethicin and analogues. *Proc. 6th Am. Peptide Symp. (in press)*

Knoll, W. 1978. Laser-Raman studies of artificial lipid membranes. Meeting of the German Biophysical Society. Ulm, F.R.G.

Kopp, F., Fringeli, U.P., Günthard, Hs.H., Mühlethaler, K. 1976. Spontaneous rearrangement in Langmuir-Blodgett layers of tripalmitin studied by means of ATR infrared spectroscopy and electron microscopy. *Z. Naturforsch.* **30c**:711

Kopp, F., Fringeli, U.P., Mühlethaler, K., Günthard, Hs.H. 1975. Instability of Langmuir-Blodgett layers of barium stearate, cadmium arachidate and tripalmitin, studied by means of electron microscopy and spectroscopy. *Biophys. Struct. Mechan.* **1**:75

Schindler, H. 1979. Autocatalytic transport of the peptide antibiotics suzukacillin and alamethicin across lipid membranes. *FEBS Lett.* **104**:157

Trifonov, A., Nikolov, P., Kolev, D., Tsenov, I. 1975. An investigation of liquid penetration through solid phase by attenuated total reflection spectroscopy (ATR). *Phys. Status Solidi* (A) **27**:135

Received 8 October 1979